Hindawi
Shock and Vibration
Volume 2021, Article ID 6680928, 14 pages
https://doi.org/10.1155/2021/6680928

Research Article

Mechanism and Prevention and Control of Mine Earthquake in Thick and Hard Rock Strata considering the Horizontal Stress Evolution of Stope

Ming Zhang[1,2] **Xuelong Hu**[1] **Hongtao Huang**[3] **Guangyao Chen**[3] **Shan Gao**[3] **Chao Liu**[3] **and Lihua Tian**[4]

[1]*State Key Laboratory of Mining Response and Disaster Prevention and Control in Deep Coal Mines, Anhui University of Science and Technology, Huainan 232001, China*
[2]*State Key Laboratory of Coal Resources and Safe Mining, China University of Mining and Technology, Xuzhou 221116, China*
[3]*Weishan Jinyuan Coal Mine, Jining 277600, China*
[4]*Gaozhuang Coal Industry Co., Ltd, Zaozhuang Mining Group, Jining 277605, China*

Correspondence should be addressed to Ming Zhang; ok_ming_ming@126.com

Received 31 December 2020; Revised 4 February 2021; Accepted 9 February 2021; Published 20 February 2021

Academic Editor: Guangchao Zhang

This study investigated the mechanism, prevention measures, and control methods for earthquake disasters typically occurring in mines with thick and hard rock strata. A mine stope with large faults and thick hard rock strata in Hebei Province was taken as the background study object. Then, theoretical analysis and numerical simulation methods were adopted in conjunction with field monitoring to explore how horizontal stress evolves in the thick and hard hanging roofs of such mines, potentially leading to mining earthquakes. Then, based on the obtained results, a mining design method was proposed to reduce the horizontal stress levels of earthquake mitigation. The results showed that, under the control of large faults, semiopen and semiclosed stopes with thick hard rock strata are formed, which cause influentially pressurized and depressurized zones during the evolution of the overburden movements and horizontal stress. It was determined that the stress concentrations mainly originated from the release and transfer of horizontal stress during the rock fractures and movements in the roof areas, which were calculated using a theoretical estimation model. The horizontal stress concentrations formed "counter torques" at both ends of the thick and hard strata, which prevented the support ending due to tensile failures. As a result, the limit spans were increased. This study proposed a mining strategy of using narrow working faces, strip mining processes, and reasonable mining speeds, which could effectively reduce horizontal stress concentrations and consequently prevent and control mining earthquakes. This study's research results were successfully applied to the mining practices in working face 16103.

1. Introduction

In many mining areas of Shandong, Henan, Anhui, Hebei, and other provinces, thick and hard rock strata exist which are characterized by great thicknesses, high strength levels, and good integrity [1–3]. The fracture movements of thick and hard rock strata overlying mining stopes can potentially cause different degrees of mining earthquakes and induce dynamic behaviors, such as rock bursts. At present, according to the incomplete statistical records, nearly 187 coal mines have been affected by mining earthquake disasters in China [4]. The accidents in some mines, such as rock bursts caused by strong mining earthquakes induced by thick and hard rock strata movements, are serious and difficult to control. These disasters have affected mine safety and production and restricted the harmonious development of some mining areas [5]. For example, on February 28th of 2010, a 2.8 magnitude (energy: 1.28×10^7 J) mining earthquake occurred at a location 70 m from the belt roadway advance in the No. 2103 longwall mining face of the Gucheng Coal Mine in Shandong Province. The mining earthquake induced a rock burst accident which damaged

260-meter-long roadway, and strong earthquake effects could be felt in the mining area and nearby village. The subsequent analysis of the accident showed that there was a 114.2 m thick medium-grained sandstone formation located at 504 m above the coal seam, and the mining earthquake caused by the fracturing of that layer had been the main cause of the rock burst accident [6], as shown in Figure 1(a). Similarly, on November 3rd of 2011, a strong mining earthquake (energy: 3.5×10^8 J) was induced by the movements of a hugely thick conglomerate (thickness of approximately 500 m) in the No. 21221 excavation roadway heading face of the Qianqiu Coal Mine in Henan Province. The earthquake was felt strongly on the ground in the mining area and had also induced a rock burst accident. The roadway suffered serious crushing and collapse actions that blocked or buried the working miners. The results included 10 deaths and 64 injuries, with direct economic losses of nearly 100 million yuan [7], as shown in Figure 1(b).

With the continuous depletion of shallow coal resources and the gradual increases in mining intensity and depth, the frequency and risks of mining earthquakes and their induced rock burst disasters will increase dramatically. Many experts and scholars have carried out research related to effective prediction and prevention measures for mining earthquakes. For example, Urbancic and Trifu [8] summarized mine earthquake monitoring technology and earthquake source type identification methods and proposed a method for predicting the effects of mining earthquakes using vibration velocity and acceleration. Also, combined with microseismic monitoring results, Lebeau et al. [9] analyzed the cause of a mining earthquake with 3.6 magnitudes in Meilai Bahe and established the relationships between the mine's seismic activity, stope stress levels, and elastic energy release rate. Nordström et al. [10] analyzed the earthquake source parameters of 46 mining earthquakes which had induced by mining activities based on the Brune Model, the distribution laws of the different earthquake source parameters were calculated, and the relationships between the source parameters and the forms of hard rock damages were identified. In another related study, Konicek [11] introduced a process of using blasting methods to control mining earthquakes in the thick and hard roof areas of the Upper Silesian Coal Basin. It was determined that roof fractures from blasting operations could potentially weaken the elastic energy of the hard rock roofs and surrounding rock and effectively reduce mining earthquake disasters and hydraulic support pressure during longwall mining processes. Qian et al. [12] introduced a key stratum theory and a masonry beam theory, which provided a theoretical basis for the study of the formation and instability laws related to the spatial structures of the thick and hard rock strata in stopes. Dou et al. [13] used a microseismic monitoring method to analyze the influence effects of the state of thick and hard rock strata on the formations and distributions of overburden structures and then built a mine earthquake prediction model of the OX-F-T structures of thick and hard rock strata. Xu et al. [14] selected the Yangliu Coal Mine as an example to analyze a theoretical model of energy release and propagation attenuation of mining earthquakes induced by the fracture movements of thick and hard rock strata. In the aforementioned study, gas disasters induced by mining earthquakes were successfully forecasted and verified. Li et al. [15] simulated the propagation of fracture-type mining earthquake sources in thick and hard rock strata using similar material through physical testing methods and established the relationships between the earthquake sources and the vibration intensity factors, such as amplitude, velocity, and acceleration.

The existing research results can be used to explain the relationships between the movements of thick and hard rock strata and mining earthquakes and can also provide guidance for prevention and control measures for underground disasters. However, the relevant research results were mainly based on the special conditions or basic assumptions of the examined mines. However, since the occurrence mechanisms and types of mining earthquakes in different mines are known to be complex and variable, the main solution to these types of problems would be to carry out specific research according to the actual mining conditions.

It has been confirmed that the relationships between the overburden fracture movements and stress evolution of the mining stopes [16] are significant problems in the field of mining production. The fracture ranges and stress concentrations of the overburden rock formations are closely related to the movement states of thick and hard rock strata in a mining area. Therefore, for mining stopes with strata obviously affected by horizontal stress conditions (such as large fault structures), the fracture movements of the mining overburden will tend to release and transfer localized horizontal stress in the stopes. Therefore, it is necessary to analyze the evolution law of horizontal stress in mining stopes. In previous studies, the influences of the horizontal stress evolution on the movements of thick and hard rock strata inducing mining earthquakes have not been deeply considered. Therefore, given the current situation, a typical large fault-controlled stope of a mine in Hebei Province was selected in this study as the research focus. The release and transfer mechanisms of the horizontal stress in the selected large fault-controlled stope were analyzed using a quantitative estimation method. The horizontal concentration force of both the open strata and the thick and hard rock strata were analyzed, and a simplified model of a mining earthquake in thick and hard rock strata affected by horizontal stress was established on that basis. Finally, a mining earthquake occurrence model for a hanging roof composed of thick and hard rock strata in a stope, as well as a shock absorption mining method, was introduced. The results achieved in this experimental study will potentially provide a theoretical basis for the safe mining of working faces under such conditions in the future.

1.1. Introduction of the Research Background. The No. 6 coal seam in a stope of a mine in Hebei Province is located in the middle of a Taiyuan formation. The surface is located in a vein of Taihang Mountain. The mining depth ranges between 250 and 400 m, and the coal thickness in the No. 6 coal seam ranges between 6 and 8 m, with a dip angle of

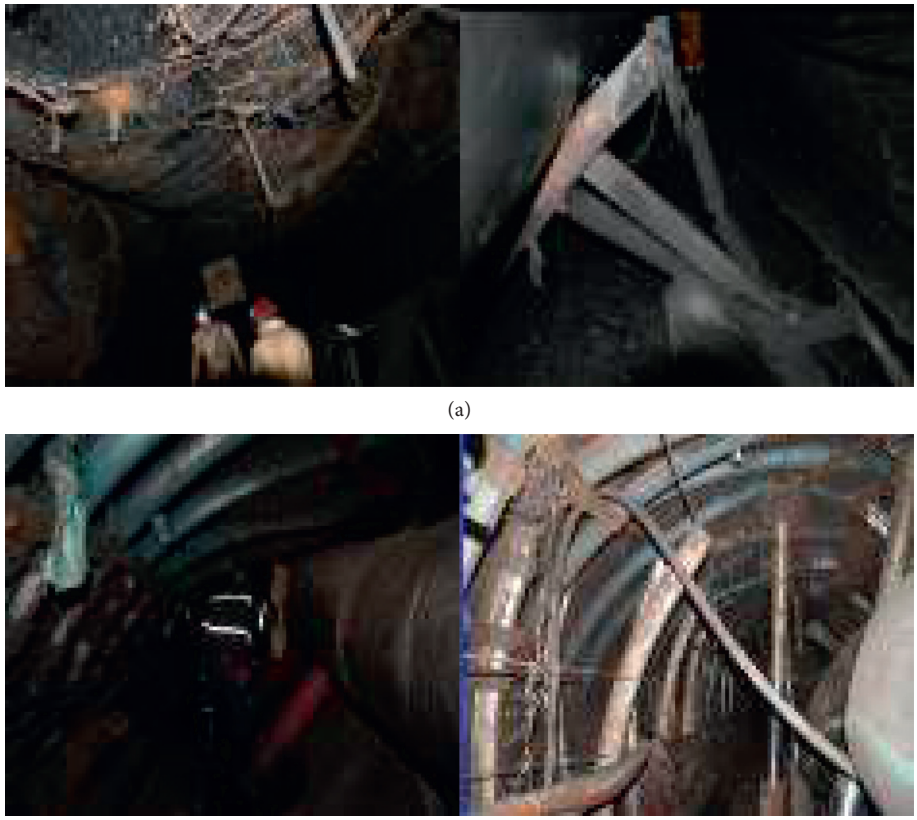

(a)

(b)

Figure 1: Typical mine earthquake disaster results caused by thick and hard rock strata movements. (a) Site image of a "2.28" mine earthquake disaster in the Gucheng Coal Mine of Shandong Province. (b) Site image of an "11.3" mine earthquake disaster in the Qianqiu coal mine of Henan Province.

approximately 6 to 15°. The first mining face (16101) is located in front of an old goaf on the north wing of the mine, as shown in Figure 2. The cutting hole is far away from the old goaf. The inclined length of the working face is 150 m, and the strike length is approximately 770 m. The mining technology of a longwall mining method is primarily used. Also, fully mechanized mine caving and stope technology and a total caving method have been adopted for the management of the roof boards. There are two groups of thick and hard key strata composed of limestone and igneous rock in the upper part of the No. 6 coal seam. The thickness of the lower limestone is approximately 30 m, and the distance between the low limestone and the No. 6 coal seam is estimated at approximately 45 m. At the top of the limestone layers, a very large thickness of igneous rock (approximately 180 m thick) directly occurs. The primary detection processes have indicated that igneous rock covers the entire mining area to varying degrees. Two large faults are distributed on both sides of the mining area, which are referred to as F7 (difference of level approximately 250 m) and FN (difference of level more than 200 m), respectively. Based on the drilling data of the strata section, these large faults cut through the roof strata. As shown in Figure 3, the strata around the faults are obviously affected by magmatic rock intrusions and crustal movements, forming approximate horizontal extrusion effects. The actual mining

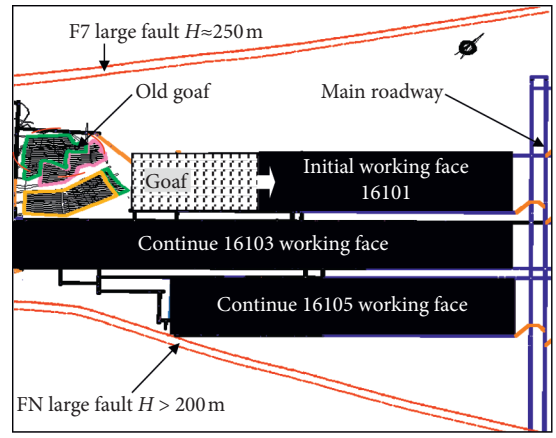

Figure 2: Layout plan of the initial working face (16101).

processes and ground stress test results have indicated that the horizontal stress levels of coal and rock around the mine's working face are high.

During the early stoping stage of the initial mining of the first working face (16101), the limestone layers experienced "hanging roof" phenomena. However, the ground and underground areas were found to be relatively stable. When the working face was pushed to approximately between 200 to 220 m away from the cutting hole, the movement activities

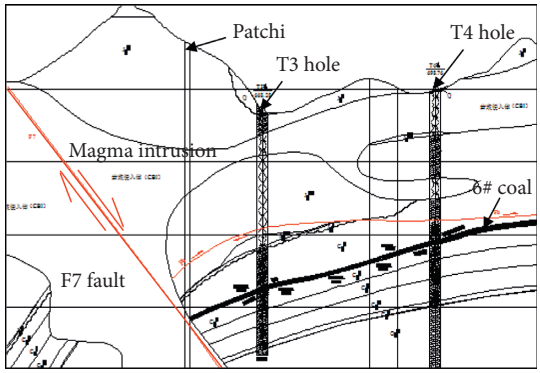

Figure 3: Intrusion and compression effects of magmatic rock in large faults.

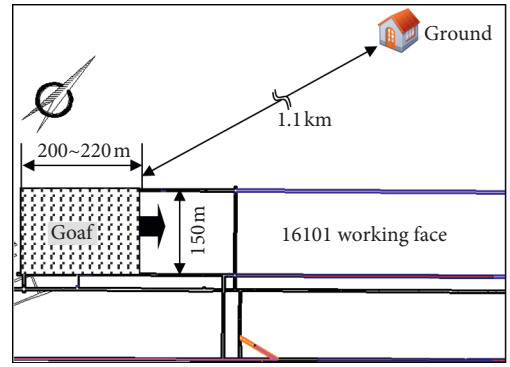

Figure 4: Schematic diagram of ground impacts caused by mining earthquakes in working face 16101.

of the limestone layers were obviously intensified and finally experienced fracture activities resulting in strong underground dynamic events and different degrees of ground earthquake effects. The strong mine earthquakes caused ground vibrations in nearby villages within a range of 1.1 km (plane distance) from the boundary of the working face, as shown in Figure 4. These strong mine earthquake events caused the villagers to panic. Some of their houses were deformed and damaged by the earthquake effects, which had once led to the stoppage of the mining activities. After the working face resumed production, the "hanging roof" phenomena of the limestone once again appeared after a certain distance. Then, with the advancement of the working face, several mine earthquakes of different degrees occurred, which included ground "shaking" actions. The "hanging roof" of limestone and its movements induced the aforementioned mining earthquakes and presented major potential safety hazards to the mine's production activities. Therefore, it is urgent to study the causes of "hanging roofs" in mines and design shock absorption methods for the thick hard rock strata (for example, limestone) overlying the stopes of operating mines in order to control the movements of limestone within the safe production range of the working faces.

1.2. Stope Space Model of Semiopen and Semiclosed Thick Rock Strata considering the Effects of Horizontal Stress. This study selected the 16101 working face of a mine in Hebei Province as an example. It was found during the mining processes that the rock surrounding the mining roadways (roughly parallel to the fault trace) were subject to the strong squeezing effects of horizontal stress due to the control of large faults on both sides, and the roadway floors buckled or bulged to different degrees. In this study, based on the comprehensive analyses of the effects of large faults and magmatic rock intrusions, it was inferred that, under the long-term actions of gravity and the controlling effects of the faults, a horizontal stress field had formed in the surrounding area of the large faults perpendicular to the fault trace. In addition, the high horizontal stress had far-reaching influences on the layered strata, which was determined to be the main reason for the deformations of the roadways. Therefore, it was considered that the horizontal stress of the stope should be considered when examining the roof movements of the working face in the study area.

Since the horizontal stress naturally exists around stopes and cannot disappear without a foundation, the fracture movement processes of the overburden of the mining were also the processes of the local horizontal stress release and transfer. In order to further study the relationship between mining overburden movements and the horizontal stress evolution, this study simplified the stope conditions, as well as the original horizontal stress distribution characteristics. Then, based on the relationships between the stratum characteristics and the mining scale of the working face, this study put forward a simplified semiopen and semiclosed stope space model which considered the influences of the horizontal stress levels, as shown in Figure 5.

In addition to the mining depths, the simplified model also included the indirect influences of the strata and horizontal stress outside the range of the strata surrounding the stopes. In the model, the hanging wall strata extruded with the footwall of the fault under self-weight conditions, and the section was perpendicular to the strike of the fault (taking the hanging wall of the fault as an example). Then, by taking rock strata with arbitrary unit thickness as the research object, which was located in the hanging wall of the fault and was in contact with the footwall of the fault, a distribution diagram of the stress of the rock strata around the fault was obtained, where $F_{\perp}$ represents the total counter force of the footwall of the fault acting on the thick and hard rock strata and other units. Then, in accordance with the vector synthesis and decomposition, $F_{\perp}$ could be decomposed into the force F_x parallel (horizontal) to the surface of the rock strata and the force F_y perpendicular (vertical) to the surface of the rock strata. Therefore, under this stable static condition, the vertical force F_y and the dead weight of the rock strata were mutually balanced. For the stope strata dominated by sedimentary rock, the horizontal force F_x was found to have a major influence on the movements of the layered strata. However, due to the complex and variable geological conditions, the actual horizontal stress distribution needed to consider factors such as lithology and structure. Since the distribution characteristics are also very complex, the accuracy of

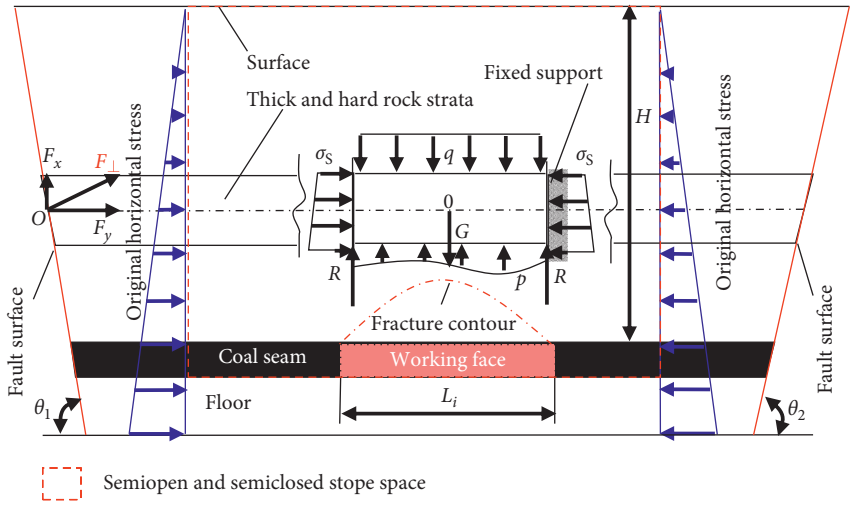

Figure 5: Semiopen and semiclosed stope space model considering the influences of the horizontal stress.

horizontal stress levels and distributions are known to be difficult to estimate. At present, experts and scholars mainly use in situ tests combined with statistical analyses to obtain the levels and directions of horizontal stress. The relevant research results [17, 18] have indicated that the horizontal principal stress levels of the shallow-middle deep strata in China are approximately 0.8 to 3.3 times those of the vertical principal stress levels. When mining depths reach or exceed more than thousands of meters, the horizontal principal stress levels are approximately equal to the vertical principal stress levels, with an overall trend of the horizontal stress gradually increasing with increases in the mining depths. In order to highlight the main contradictions and facilitate the research, the results mentioned in [17, 18] were consulted. In this study, the horizontal stress was considered to be approximate to the gradient function of the mining depth, which took 0 on the ground as the initial value and presented a linear relationship with the increases in the mining depths.

2. Evolution Law and Qualitative Analysis of the Horizontal Stress Levels in the Stopes

2.1. Release and Transfer of the Horizontal Stress in the Stopes as Revealed by Numerical Simulations. The horizontal stress in the stope space model of this study's semiopen and semiclosed thick hard rock strata demonstrated a certain evolutionary law with the mining of the working face under the constraints of "clamping" control of the large faults. FLAC3D software was used for numerical simulations and qualitative disclosures in this study. The model was divided into 13, 320 cells and adopted a Mohr–Coulomb failure criterion. The relevant rock parameters are detailed in Table 1. A coal pillar boundary measuring 225 m was reserved on the left side, and a 225 m coal pillar boundary was reserved on the right side of the excavation face. The pillar heights were 340 m, and the working face had a width of 150 m. The horizontal displacement constraint is used on the left and right boundaries to simplify and replace the constraint effect of "clamping" from the large fault. In addition, the horizontal and vertical bidirectional displacement constraints were used for the bottom boundary. Then, in order to highlight the various characteristics of the horizontal stress during mining activities, the ratio λ (lateral pressure coefficient) of the horizontal stress to the vertical stress is set to be 1.5. The established model is shown in Figure 6.

After the working face was extracted, the roof strata at all levels of the stope had fractured from the bottom to top (floor strata from the top to bottom), corresponding to the strata of the plastic zone shown in Figure 7(a). The horizontal stress in the roof fracture zone decreased significantly from original horizontal stress of 16.50 to 18.75 MPa to between 1.66 and 8.99 MPa, forming the horizontal stress "depressurization zone" corresponding to the rock strata at the edge of the plastic zone shown in Figure 7(b). The decreases in horizontal stress had mainly occurred in the fracture areas of the roof strata. However, the horizontal stress in the floor areas of the working face had also decreased to some extent. The horizontal stress of the limestone increased from an initial 12.75 to 16.50 MPa to between 18.11 and 23.81 MPa. Therefore, with the horizontal stress levels obviously increased, a "pressurization area" of horizontal stress was formed. The limestone became the "key layer" or "bearing layer" under the concentrated effects of the horizontal stress. It was predicted that the influence ranges and degrees of the horizontal stress "depressurization area" and "pressurization area" would further increase with increases in the range of the working face.

It was observed in this study that, without the inflow of an external force source, the stress in the model would not disappear and produce without foundation. In theory, the horizontal stress in the "pressurization area" should mainly originate from the release, transfer, and concentration of the horizontal stress in the "depressurization area," and the stress levels in the "pressurization area" and "depressurization area" would maintain an internal balance. Therefore, there were internal mechanisms for the release and transfer of horizontal stress and the horizontal stress concentrations

Table 1: Mechanical parameters of the rock model.

Type of rock strata	Thickness (m)	Unit weight (kN•m^{-3})	Modulus of elasticity (GPa)	Internal friction angle (°)	Tensile strength (MPa)
Topsoil	75.0	18	14.5	22	1.4
Igneous rock	180.0	27	30.5	40	6.5
Limestone	30.0	27	22.5	37	4.1
Sandy mud interbedding	38.0	24	16.5	29	2.9
Carbonaceous mudstone	7.0	20	14.5	24	2.0
No. 6 coal	7.0	14	13.5	20	1.7
Sandstone	3.0	25	15.5	25	2.2

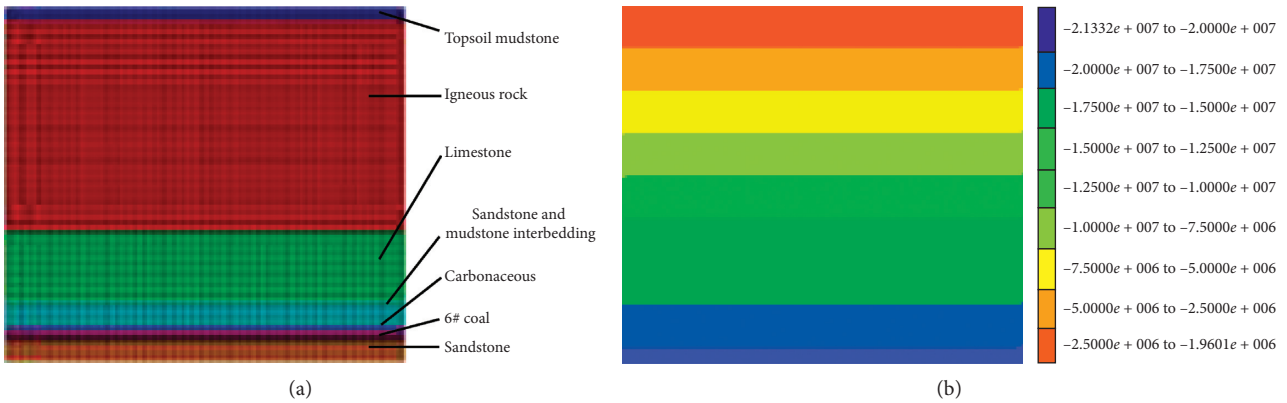

Figure 6: FLAC3D numerical analysis model. (a) Cell divisions. (b) Initial horizontal stress distribution.

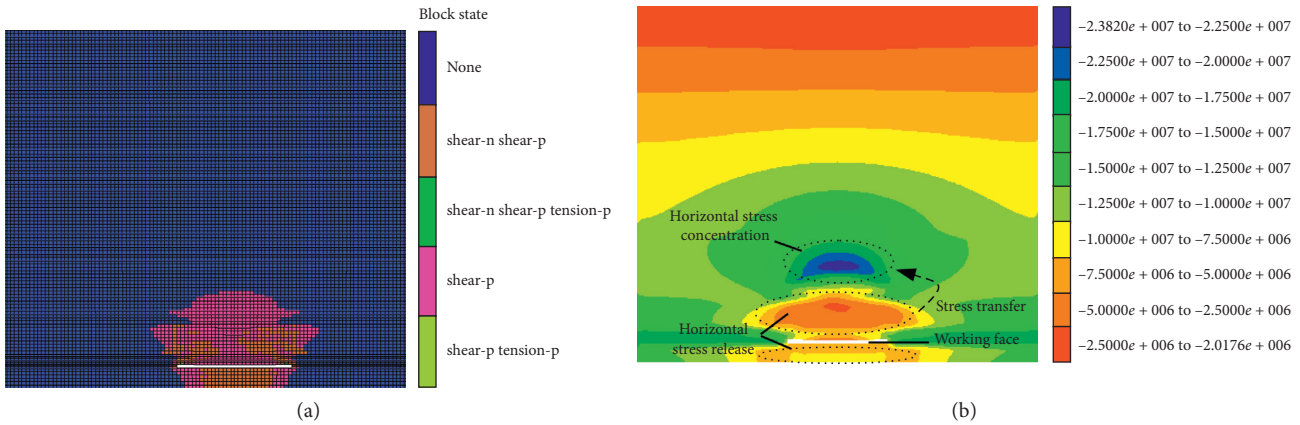

Figure 7: Distribution characteristics of the plastic zone and horizontal stress of the rock surrounding the stope. (a) Distribution of the plastic zone. (b) Distribution of the horizontal stress.

of the "bearing stratum" during the mining process of the working face.

2.2. Quantitative Analysis of Horizontal Stress Transfer in the Height Direction of the Stope. The key stratum theory holds that the movements of the overlying strata in a stope are in the basic unit of the rock stratum group. The hard rock strata in each group of the rock strata are the key strata which control the movements or deformations of the group of strata and are also the concentrated strata (or bearing stratum) of the horizontal stress. According to the microseismic monitoring results [19], the fracturing processes of hard rock stratum last only tens to hundreds of milliseconds. At the same time, with the fracture movements of the thick and hard rock strata, the majority of the horizontal stress accumulated in the original hard rock strata will be released and transferred to the thick and hard rock strata in the adjacent rock formations in only an instant, forming a new horizontal stress balance. However, with the continuous

advancement of mine working faces (goaf range gradually increasing), the overlying strata of a stope will fracture layer by layer. The processes of fracturing and horizontal stress transference of the above hard strata will continue to repeat until the fracturing height reaches that of the thick hard strata and forms horizontal stress concentrations in the key rock strata. Therefore, a simplified theoretical model of the horizontal stress release and transfer processes in the vertical direction was established to semiquantitatively analyze the evolution process of the horizontal stress in the above-mentioned mining area, as shown in Figure 8.

It was assumed that the hard rock stratum was fractured layer by layer, and the majority of the released horizontal stress was mainly transferred to the adjacent unbroken hard rock stratum. In the current study, h_1, h_2, h_3, and h_4 denote the thicknesses of each hard rock stratum, respectively, m; σ_1, σ_2, σ_3, and σ_4 represent the initial horizontal stress levels of each hard rock stratum group, MPa, as shown in Figure 8(a), and the corresponding σ_2', σ_3', and σ_4' are the concentrated horizontal stress levels prior to the fracturing of each hard rock stratum during the mining process, MPa. It can be seen in Figure 8(b) that when the first working face was stoped (or the goaf area was small) and when the first group of hard rock stratum fractured, the majority of the horizontal stress was transferred to the adjacent second group of hard rock stratum. Then, by assuming that the transfer coefficient of the horizontal stress from the first group of hard rock stratum to the second group of hard rock stratum was a_1 following the fracturing of the first group of hard rock stratum, the accumulated horizontal stress σ_2' of the second group of hard rock can be written as follows:

$$\sigma_2' = \sigma_2 + a_1\sigma_1\frac{h_1}{h_2}. \tag{1}$$

In the same way, during the stoping of the second and third working faces, if the transfer coefficients of the second and third groups of hard rock stratum were a_2 and a_3, respectively, then the concentrated horizontal stress σ_3' and σ_4' of the second and third groups of hard rock stratum can be obtained as follows:

$$\begin{aligned}\sigma_3' &= \sigma_3 + a_2\sigma_2'\frac{h_2}{h_3},\\ \sigma_4' &= \sigma_4 + a_3\sigma_3'\frac{h_3}{h_4}.\end{aligned} \tag{2}$$

Then, by summarizing the horizontal stress transfer law of the stope, the concentrated horizontal stress σ_n' prior to the fracturing of the hard rock strata in group n can be obtained according to formulas (1) and (2) as follows:

$$\sigma_n' = \sigma_n + \frac{h_1\sigma_1}{h_n}a_1, \ldots, a_{n-1} + \cdots + \frac{h_{n-1}\sigma_{n-1}}{h_n}a_{n-1}. \tag{3}$$

Therefore, it can be seen that the horizontal stress of any group of hard rock strata is formed by the superposition of the original horizontal stress and the horizontal transfer stress caused by the mining activities. It can then be inferred that the higher the original horizontal stress, the larger the mining scale (overburden fracture range) and the farther the thick hard rock strata from the coal seam. As a result, the horizontal stress concentrations of the thick hard rock strata will be more obvious.

3. Simplified Mining Earthquake Model for Estimating the Horizontal Concentrated Force of the Thick and Hard Rock Strata in a Stope and Its Influencing Effects

3.1. Estimations of the Horizontal Concentrated Force of Thick and Hard Rock Strata in a Stope. This study's comprehensive numerical simulation and quantitative analysis results of horizontal stress transfer showed that a certain relationship existed between the overburden movements and the evolution of horizontal stress. This study further analyzed and estimated the horizontal concentrated force of the high-level thick and hard strata.

Due to the influences of the plate movements, topography, geological structures, and creep of the rock masses on the shallow parts of the Earth's crust, the distribution laws of in situ stress fields are complex and variable. However, they are known to present an overall trend of gradual increases in horizontal stress levels with increases in buried depths. For this reason, it was assumed in this study that the horizontal stress distribution in the stope was approximately linear, as shown in Figure 9. As can be seen from formula (3), following the mining of the working face, the horizontal stress σ_s of any unbroken rock strata overlying the goaf was the superposition of the original horizontal stress σ_h and the horizontal transfer stress σ_Δ caused by the mining activities as follows:

$$\sigma_s = \sigma_h + \sigma_\Delta, \tag{4}$$

$$\sigma_h = \lambda\gamma h, \tag{5}$$

where λ is a constant related to the rock stratum, the surrounding environment of the stope, and so on. In a uniform rock body, $\lambda_0 = u/(1-u)$ under the state of self-weight stress and u is Poisson's ratio of the rock stratum. Therefore, when considering the influences of the structure on the stope, if Poisson's ratio is constant, then the calculation formula of the horizontal lateral pressure coefficient is $\lambda = K\lambda_0 = Ku/(1-u)$, and the horizontal stress concentration coefficient is generally $K > 1$. γ is the average unit weight of the overburden, kN/m^3. h is the buried depth of the rock layer, m.

The mining scales of a single working face or a first mining face tend to be small. In addition, the overhanging span of the bottoms of the thick and hard layers is also small and may not reach ultimate fracture spans. However, with increases in the goaf area, the thick and hard rock strata may remain relatively stable and prevent the upward development of fracture height in the high direction (or "thick and hard rock strata effect platforms"). However, due to the fracturing of the low-level and floor strata during the mining processes, the horizontal stress concentrated in the original

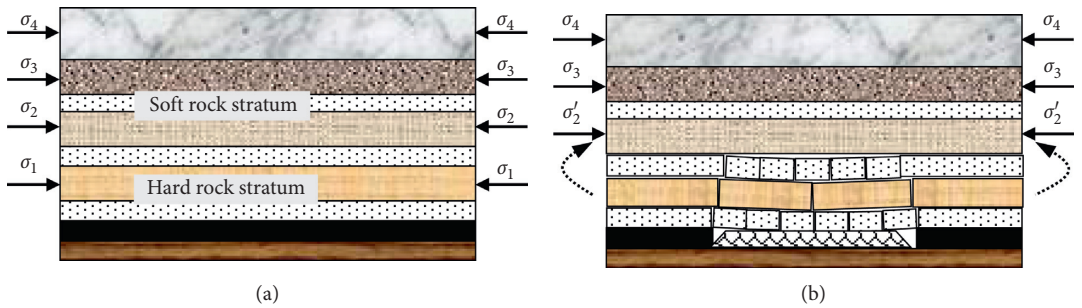

Figure 8: Horizontal stress distribution and transfer model in the vertical direction. (a) Distribution of the initial horizontal stress. (b) Upward transference of the horizontal stress.

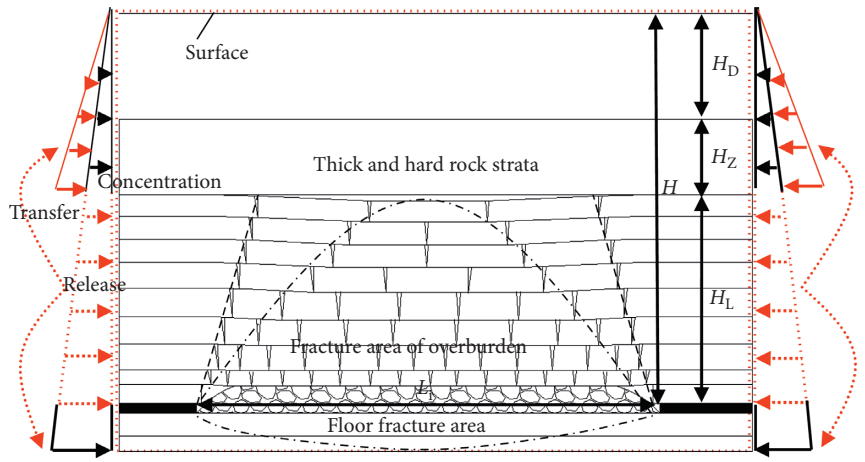

Figure 9: Simplified model of the overburden fractures and horizontal stress transfer in the stope.

bearing layers will be released and transferred to the key strata without fractures occurring. Therefore, the excavations of working faces include two processes: overburden fracturing and horizontal stress release and transfer.

Before the strata enter the full mining stage, the maximum fracture height of the overlying strata in the stope will be approximately half of the length of the short side of the goaf [20]. Generally speaking, the maximum fracture height of a working face is related to the length of the short side of the goaf or the inclined length or advance distance of the working face. Prior to the fracturing of thick and hard rock strata, the maximum fracture height of the overlying strata in a stope is $H_i = \eta_1 L_i$, where L_i is the width of the short side of the goaf and η_1 is the fracture height coefficient of the overburden as determined by different mining technologies and geological conditions. The fracture depth of the floor strata will be $D_i = \eta_2 L_i$, where η_2 is the fracture depth coefficient of the floor as determined by different mining technologies and geological conditions. When the fracture height of the overburden reaches the occurrence height of the thick and hard rock strata (for example, $H_i = \eta_1$ and $L_i = H_L$), the fracture height of the overburden no longer develops upward due to the "platform effects of the thick and hard rock strata." The horizontal stress levels of the thick and hard strata will remain relatively unchanged. Then, the horizontal concentration force P released by the fractures of the overburden can be expressed as follows:

$$P = \int_{H-H_L}^{H} \lambda \gamma h \, dh = \frac{\lambda \gamma}{2} (2H - H_L) H_L, \tag{6}$$

where H_L indicates the height of the thick hard rock from the coal seam, m, and H is the buried depth of the coal seam, m.

The horizontal concentrated force P "released" in the mining fracture area can be transferred to the roof and floor strata. In an ideal situation, the comprehensive transfer coefficient from the nonfractured roof to each stratum on the surface is φ (0, 1), and the rest is transferred to the floor area of the working face and transfer coefficient $1 - \varphi \in (0, 1)$. There is no clear definition of the transfer ratio to a certain key roof or bottom rock layer. In order to facilitate this study's investigations, it was assumed that the transferred horizontal stress was still distributed in a vertical linear manner, and the transferred horizontal stress σ_Δ of the nonfractured rock stratum was as follows:

$$\sigma_\Delta = \frac{2\varphi P h}{(H - H_L)^2} = \frac{\varphi \lambda \gamma h (2H - H_L) H_L}{(H - H_L)^2}. \tag{7}$$

Then, by substituting equations (5) and (7) into equation (4), it was determined that the superimposed horizontal stress σ_s of the thick and hard layers without fractures was as follows:

$$\sigma_S = \lambda\gamma h\left[1 + \frac{\varphi H_L(2H - H_L)}{(H - H_L)^2}\right], \tag{8}$$

where h represents the occurrence height range of the thick and hard rock strata, $h \in [H_D, H_D + H_Z]$.

Then, after the definite integration of equation (8), the calculation formula F of the horizontal concentrated force of the thick and hard rock strata could be expressed as follows:

$$F = \int_{H_D}^{H_D+H_Z} \sigma_S \mathrm{d}h = \Omega \cdot \frac{\lambda\gamma\ (2H_D + H_Z)H_Z}{2}, \tag{9}$$

where $\Omega = 1 + ((\varphi H_L(2H - H_L))/(H - H_L)^2)$.

The horizontal concentrated force F of thick and hard rock strata is not only determined by the specific stope conditions but also closely related to the stope scale (mining range). The fracture heights and depths of the overburden and floor are determined by the goaf range and the mining degrees of the different working faces. In this study, strata structure analysis and field monitoring method were adopted, and the relevant parameters were obtained. Then, the horizontal concentration force of the key strata was quantitatively estimated.

3.2. Simplified Model of Mining Earthquakes in Thick and Hard Rock Strata considering the Horizontal Stress. In previous studies, the key strata near a stope were simplified to fixed beams or simply supported beams in the examinations of using roof type mine earthquake models. However, the horizontal stress concentration effects were not considered in the models. Similarly, in this study's background study area, it was found that, under the influences of the control effects of the large faults, the thick and hard rock strata were obviously affected by horizontal stress transference and concentrations during the mining processes, and these factors could not be completely ignored in theory. Therefore, in order to reflect the main contradictions, a simplified mechanical model of the fixed support beams of thick and hard rock strata under horizontal stress conditions was established in this study according to the Saint Venant Principle, as detailed in Figure 10.

When the thick and hard beams became bent and deformed, bending strain energy corresponding to the bending deformations and shear strain energy corresponding to the shear deformations were both observed. The influence effects of the shear deformations on the displacements are usually very small and generally ignored in engineering. When a rock beam becomes bent, its length is dx, and the bending strain energy values in the small deformations can be obtained as follows:

$$\mathrm{d}U_x = \frac{M_x}{2}\mathrm{d}\theta = \frac{M_x^2}{2}EI\mathrm{d}x, \tag{10}$$

where E is the elastic modulus of rock beam, GPa, and I denotes the moment of inertia of the rock beam section per unit width, m^4, $I = (H_Z^3/12)$.

When a rock beam is bent, the storage strain energy in its full-length range is

$$U = \int_0^L U_x \mathrm{d}x = \frac{EI}{2}\int_0^L \left(\frac{\mathrm{d}y^2}{\mathrm{d}^2x}\right)^2 \mathrm{d}x. \tag{11}$$

Then, the work done during the bending process by the vertical uniform load q of the rock beam is

$$U_q = q\int_0^L y\mathrm{d}x. \tag{12}$$

The work done to the rock beam by the horizontal concentrated stress F is

$$U_F = \frac{F}{2}\int_0^L \left(\frac{\mathrm{d}y}{\mathrm{d}x}\right)^2 \mathrm{d}x. \tag{13}$$

In accordance with the conservation of energy conversion, the total energy stored during the bending process of the rock beam will be as follows:

$$\delta = U - U_q - U_F. \tag{14}$$

In addition, according to the boundary conditions of the model, $y|x = 0 = 0$和$y|x = L = 0$, and the maximum deflection at the middle part of the suspended span of the rock beam will be w. That is to say, $y|_{x = L/2} = w$. Then, the deflection curve equation will be established using a Rayleigh–Ritz method [21]:

$$y = w\sin\frac{\pi x}{L}. \tag{15}$$

The partial differential function $(\partial\delta/\partial w)$ of the total energy δ with respect to $w$is equal to 0.

Then,

$$\frac{\partial\delta}{\partial w} = \frac{\partial\left(\left(\left(\pi^4 w^2 EI\right)/4L^3\right) - ((2qwL)/\pi) - \left(\left(F\pi^2 w^2\right)/4L\right)\right)}{\partial w}$$

$$= \frac{\pi^4 wEI}{2L^3} - \frac{2qL}{\pi} - \frac{F\pi^2 w}{2L} = 0. \tag{16}$$

Therefore, it can be concluded that the w expression is

$$w = \frac{4qL^4}{\pi\left(\pi^4 EI - F\pi^2 L^2\right)} \approx \frac{5qL^4}{384EI}\cdot\frac{F_C}{F_C - F}, \tag{17}$$

where $5qL^4/384EI$ is the maximum deflection of the rock beam under vertical uniform load q and the Euler constant is $F_C = \pi^2 EI/L^2$. Therefore, under the conditions of horizontal concentrated stress and vertical uniform loads, the maximum bending tensile stress per unit section of rock beam and the condition of no fracture is as follows:

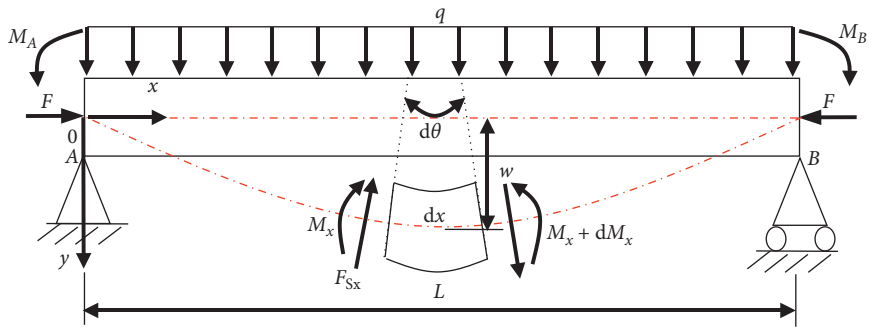

Figure 10: Simplified model of the fixed support rock beams undergoing the effects of horizontal concentrated force.

$$\sigma_m = \frac{6M_m}{H_Z^2} - \frac{F}{H_Z} \le [\sigma], \tag{18}$$

where σ_m is the maximum tensile stress of the section when the rock beam is bent, MPa, and $[\sigma]$ is the ultimate tensile strength of the rock beam, MPa.

According to the general failure characteristics of the long beams, the ultimate bending moment of the rock beam was first reached at the supporting end of the rock beam $x_1 = 0$ (or $x_1 = L$) or at the midspan position $x_2 = L/2$. It was found that if the corresponding bending moments were M_{x_1} and M_{x_2}, then the maximum bending moment M_m of the rock beam satisfied the following:

$$M_m = \max\left(M_{x_1} = \frac{qL^2}{12}; M_{x_2} = \frac{qL^2}{24} + Fw\right). \tag{19}$$

Next, under the actions of the concentrated horizontal stress, the limit span L of the rock beam was the minimum span value of the rock beam. Therefore, by substituting equation (19) into equation (18), the following L could be obtained:

$$L_{\min} = \min\left(\sqrt{\frac{2\left([\sigma]H_Z^2 + FH_Z\right)}{q}}; 2\sqrt{\frac{[\sigma]H_Z^2 + FH_Z - 6Fw}{q}}\right). \tag{20}$$

3.3. Causes of Mining Earthquakes Induced by the Fracturing of Thick and Hard Rock Strata in Stopes Controlled by Large Faults. There are known to be internal mechanisms of horizontal stress release, transference, and horizontal stress concentration in the "bearing stratum" of thick and hard rock strata during the mining processes of working faces. With the increases in the sizes of the working faces, the horizontal stress release of the overburden fractures and the stress concentration degrees of the key thick and hard rock strata also increase. Due to the fact that the stopes controlled by large faults are under the constraints of large faults on both sides, the horizontal stress has significant effects on the stability and movement characteristics of the thick and hard rock strata. Therefore, under those conditions, the thick and hard strata become "clamped" by the horizontal concentrated stress F on both sides, and the strata ends form a "countertorque". This can prevent the ends of the strata support from experiencing tensile failures, which will further increase the limit span. Meanwhile, the elastic energy accumulated by the deformations of the thick and hard beam may also be relatively increased. When F reaches a certain limit value, it can convert the temporarily stable large areas of the thick and hard rock strata in a roof suspension state, which will not easily collapse naturally. Then, under the influences of external disturbances (for example, mining activities), once the hanging roof structures of the thick and hard rock stratum lose stability, large amounts of stored elastic energy and gravitational potential energy will be released. This had been determined to be the main cause of dynamic disasters, such as mining earthquakes.

4. Technology for Weakening the Influence of Horizontal Stress to Promote Mining Earthquake Prevention and Control

4.1. Estimations of the Concentration Forces and Limit Spans of the Limestone. In the present study, according to the geological conditions of working face 16101, the inclined length of working face L_i was 150 m. Then, by referencing previous relevant research results, it was determined that the fracture angle of overburden in the goaf could be assumed to be $\alpha = 75^\circ$ [22, 23], and the bottom hanging size of limestone in the inclined direction (width) of the working face was as follows: $L_0 = L_i - 2H_L\cot 75^\circ = 125$ m. In addition, the thickness of limestone $H_Z = 30$ m, ultimate tensile strength $[\sigma] = 4.1$ MPa, elastic modulus $E = 22.5$ GPa, distance from the No. 6 coal seam $H_L = 45$ m, distance from the surface $H_D = 255$ m, igneous rock $H_Z' = 180$ m, elastic modulus $E' = 30.5$ GPa, distance from the No. 6 coal seam $H_L = 75$ m, and the average unit weight of the overburden $\gamma = 25$ kN/m^3. The relationship between the bending rigidity of the limestone and the igneous rock was $(EH_Z^3/12) \ll (E'H_Z'^3/12)$. Therefore, the igneous rock and limestone could be separated. That is to say, the limestone could move independently. It was assumed that the horizontal concentrated force released by the overburden fractures was generally transferred to the roof and floor areas, and the horizontal stress transfer coefficient was $\varphi \approx 0.5$. Also, according to equation (9), $\Omega = 1.16$ and $F = 2.47\lambda \times 10^8$ N. The relationship between the limit span of the limestone and the lateral pressure coefficient λ is obtained using equation (20), as shown in Figure 11. It was observed that when there was no

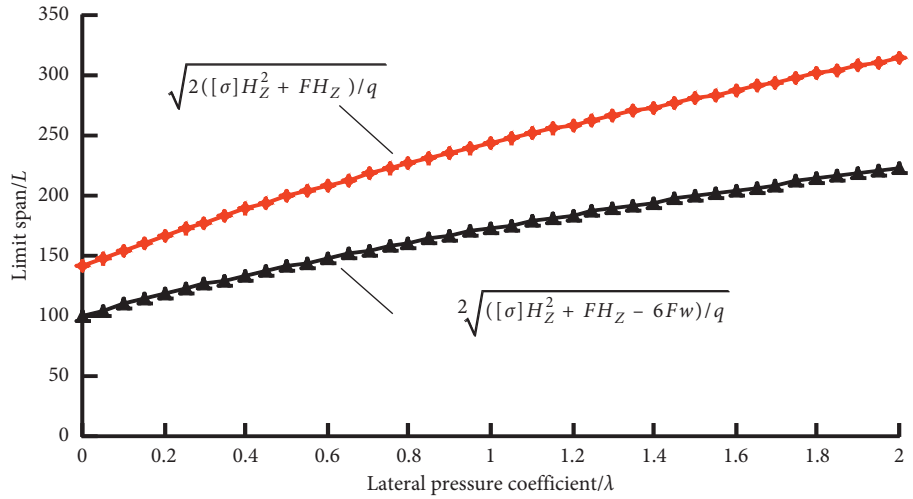

Figure 11: Different lateral pressure coefficients and limestone limit spans.

horizontal stress transference and concentration following the mining of the working face (for example, $F = 0$), the limit step distances L of the fixed support end and midpan fracture of the limestone were 100 m and 141 m, respectively, in which $L_{\min} = 100$ m $< L0 = 125$ m. Therefore, no limestone "hanging roof" structures had formed.

As detailed in Figure 11, if the limestone beams do not fracture, the corresponding minimum lateral pressure coefficient λ will be 0.3. Then, according to the Poisson ratio where u is 0.2 for the limestone, if the horizontal extrusions and control influences caused by the large faults are not considered, then K will be 1, and the lateral pressure coefficient of the limestone will be $Ku/(1-u) = 0.25$. In addition, the lateral pressure coefficient λ will be 0.3 when it is close to the ultimate fracture of the limestone. In the current study, by considering the influences of horizontal extrusions and control effects of the F7 and FN faults on both sides of the stope, when $K > 1.2$, the lateral pressure coefficient λ satisfied $\lambda = Ku/(1-u) > 0.3$. At that time, the actual span of the limestone bottom was less than its ultimate fracturing step distance, which would potentially cause a large area of "hanging roof." Therefore, the stope was considered to have been affected by the horizontal extrusions of the large faults and displayed the conditions required for the formation of limestone hanging roofs and mining earthquake events.

4.2. Shock Absorption Mining Designs and Site Monitoring Measures. In the study area, the mining design of the continuous 16103 working face had considered mining earthquake prevention and control in advance. The width design of working face 16103 had been adjusted from an original 150 m to 120 m. At the same time, the effective spacing between the strip coal pillars and the goaf of working face 16101 had been adopted, with the widths between the coal pillars measuring 80 m. These measures were used to control the maximum suspension span of the limestone within its limit fracturing step distance and avoid the fracturing of the limestone and fracture movements of the limestone, as well as the movement effects of the even higher extremely thick igneous rock caused by the mining of adjacent continuous working faces. In this study, based on the analysis results of the real-time monitoring of the installed microseismic system, the mining speed of working face 16103 had gradually increased. The average mining intensity of the actual working face was approximately 3 m/d and had not exceeded more than 5 m/d. However, if it had been found through the monitoring process that the number of times and frequency of the vibrations had increased sharply, the current mining speed would be identified as being too high. Subsequently, analysis and investigation would be carried out for stopping or slowing the mining processes in order to avoid mining earthquakes.

A BMS high-precision seismic monitoring system was installed prior to commencing mining activities in working face 16103. The number of high energy roof mining earthquake events (energy level of 10^5 J and above) was 22, and the corresponding focal heights are shown in Figure 12. There were 18 large energy mine earthquake events (82%) observed within the range of 0 to 30 m above the roof of the No. 6 coal seam and 6 large energy mining earthquake events (18%) within the range of 30 to 45 m observed above the roof of the No. 6 coal seam. Projection analysis is made on the profile of roof microseismic event in the stoping of 16103 working face. As shown in Figure 13, the roof microseismic events were concentrated in the range of 0 to 50 m above the No. 6 coal seam, and the fracture range had not exceeded the limestone occurrence height (45 to 75 m from the coal seam) as a whole. At the same time, there were no strong mining earthquakes with energy levels of 10^6 or above. It was speculated that the mining of the working face caused fracture movements in the low-level strata within a range of 0 to 45 m. Therefore, since the high-level limestone had been separated from the lower strata, it had remained relatively stable.

In the current study, it was found that, through the implementation of a narrow working face, strip mining technology, and reasonable mining intensity levels as the main shock absorption mining scheme, the surface and

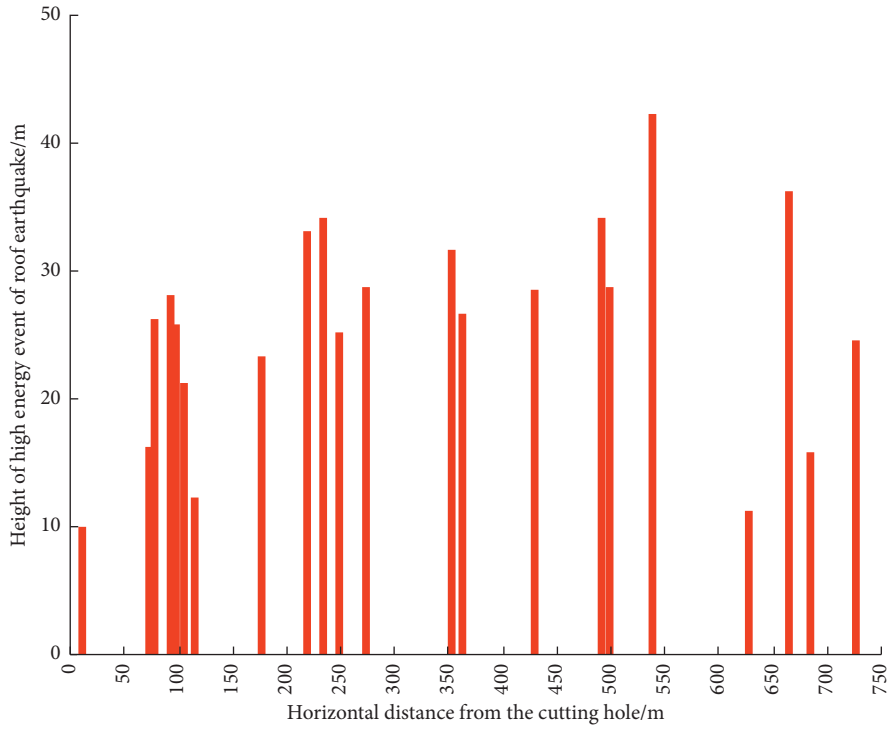

Figure 12: Statistical data of the heights of high energy mining earthquakes.

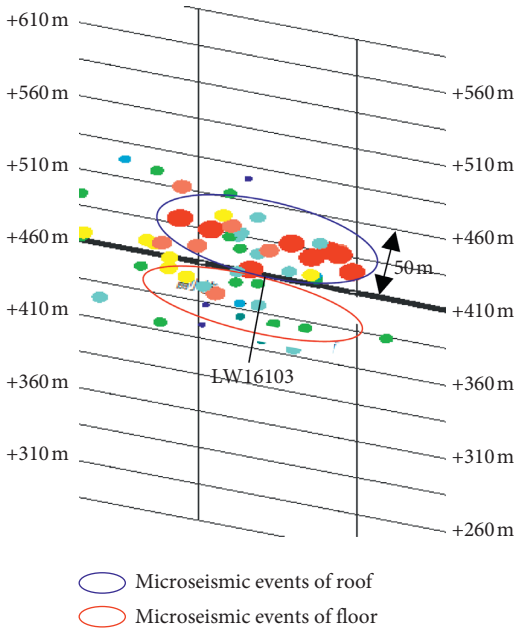

Figure 13: Profile analyses of microseismic events.

underground areas of working face 16103 had remained relatively calm during the mining processes. At the present time, the mining of the working face is considered to be completed safely, and the goals of controlling the thick and hard rock strata movements, along with the prevention and control of mining earthquakes, have been realized.

5. Conclusions

(1) Under the influence effects of large fault structures and magmatic intrusions, the horizontal square stress distributions and control effects of the stope in the study area were found to be obvious. It was observed that the thick and hard rock strata in the stope could potentially form "hanging roof" structures under the conditions of horizontal stress concentrations. Therefore, there was an enhanced possibility that the movements of the thick and hard rock strata could induce mining earthquake disasters.

(2) A space model of semiopen and semiclosed thick hard rock strata with stopes controlled by large faults was preliminarily established in this study. The basic knowledge of the internal relationships between the two main mining processes, including the overburden fracturing and horizontal stress release and transfer, was obtained. Then, the evolution law of the horizontal stress in the stope was emphatically analyzed. On that basis, a simplified analytical model for quantifying the horizontal concentrated force of thick and hard rock strata, and its estimation expressions were then established.

(3) It was found that, under the "clamping" actions of the horizontal concentrated force, the thick and hard rock beams could potentially form "countertorque" effects at the ends of the rock beams, which

would prevent the tensile failures of the supporting ends and further increase the limit span of the roof areas. This was determined to be the main mechanical mechanism of the thick and hard hanging roofs and occurrences of high energy mining earthquakes.

(4) In the study area, a mining design which included a narrow working face, strip mining technology, and reasonable mining intensities was adopted in order to reduce the influence effects of the horizontal stress evolution of the stope on the movements of the thick and hard rock strata. In addition, the magnitudes and influence degrees of the horizontal stress transference were effectively reduced, as well as the magnitudes of horizontal concentrated force at both ends of the rock beams. In summary, the adopted design had achieved the purpose of shock absorption during the mining processes. Therefore, through the aforementioned mining practices and monitoring of working face 16103, the positive safety effects of the proposed design were proven.

Data Availability

The data used to support the findings of the study are available from the corresponding author upon request.

Conflicts of Interest

The authors declare that they have no conflicts of interest.

Acknowledgments

The research was funded by the State Key Laboratory of Coal Resources and Safe Mining and CUMT, Grant/Award no. SKLCRSM21KF007, Natural Science Foundation of Anhui Province, Grant/Award no. 1908085QE186, State Key Laboratory of Mining Response and Disaster Prevention and Control in Deep Coal Mines (Anhui University of Science and Technology), Grant/Award no. SKLMRDPC19ZZ03, Anhui Natural Science Foundation of Colleges and Universities, Grant/Award no. KJ2020A0324, and Technical Innovation Project of Shandong Province, Grant/Award no. JWMQ2004-14.

References

[1] J. Wang, J. Ning, P. Qiu, Y. Shang, and H. Shang, "Microseismic monitoring and its precursory parameter of hard roof collapse in longwall faces: a case study," *Geomechanics and Engineering*, vol. 17, no. 4, pp. 375–383, 2019.

[2] M. Zhang and F. Jiang, "Rock burst criteria and control based on an abutment-stress-transfer model in deep coal roadways," *Energy Science & Engineering*, vol. 8, no. 8, pp. 2966–2975, 2020.

[3] D. Li and J. Zhang, "Rockburst monitoring in deep coalmines with protective coal panels using integrated microseismic and computed tomography methods," *Shock and Vibration*, vol. 2020, Article ID 8831351, 10 pages, 2020.

[4] Q. Qi, Y. Li, S. Zhao et al., "Seventy years development of coal mine rockburst in China: establishment and consideration of theory and technology system," *Coal Science and Technology*, vol. 47, no. 9, pp. 1–40, 2019.

[5] Y. Ding, L. Dou, W. Cai et al., "Signal characteristics of coal and rock dynamics with micro-seismic monitoring technique," *International Journal of Mining Science and Technology*, vol. 26, no. 4, pp. 683–690, 2016.

[6] M. Zhang, Y. Cheng, L. Wang, F. Jiang, and L. Qi, "Structure model and stability research of thick hard strata-coal pillar in shallow-buried re-mined panels," *Chinese Journal of Rock Mechanics and Engineering*, vol. 38, no. 1, pp. 87–100, 2019, in Chinese.

[7] Y. Jiang and Y. Zhao, "State of the art: investigation on mechanism, forecast and control of coal bumps in China," *Chinese Journal of Rock Mechanics and Engineering*, vol. 34, no. 11, pp. 2188–2204, 2015, in Chinese.

[8] T. I. Urbancic and C. I. Trifu, "Recent advances in seismic monitoring technology at Canadian mines," *Journal of Applied Geophysics*, vol. 45, no. 4, pp. 225–237, 2000.

[9] L. Trifu, F. Lahaie, M. Al Heib, J. P. Josien, P. Bigarré, and J. F. Noirel, "Seismic and geotechnical investigations following a rockburst in a complex French mining district," *International Journal of Coal Geology*, vol. 64, no. 1-2, pp. 66–78, 2005.

[10] E. Nordström, S. Dineva, and E. Nordlund, "Source parameters of seismic events potentially associated with damage in block 33/34 of the Kiirunavaara mine (Sweden)," *Acta Geophysica*, vol. 65, no. 6, pp. 1229–1242, 2017.

[11] P. Konicek and Schreiber, "Rockburst prevention via destress blasting of competent roof rocks in hard coal longwall mining," *Journal of the Southern African Institute of Mining and Metallurgy*, vol. 118, no. 3, pp. 235–242, 2018.

[12] Q. Minggao, M. Xiexing, and X. Jialin, *Key Strata Theory*, pp. 59–88, China University of Mining and Technology Press, Xuzhou, China, 2000.

[13] L.-M. Dou, X.-Q. He, H. He, J. He, and J. Fan, "Spatial structure evolution of overlying strata and inducing mechanism of rockburst in coal mine," *Transactions of Nonferrous Metals Society of China*, vol. 24, no. 4, pp. 1255–1261, 2014.

[14] C. Xu, Q. Fu, X. Cui, K. Wang, Y. Zhao, and Y. Cai, "Apparent-depth effects of the dynamic failure of thick hard rock strata on the underlying coal mass during underground mining," *Rock Mechanics and Rock Engineering*, vol. 52, no. 5, pp. 1565–1576, 2019.

[15] D. Li, J.-F. Zhang, C. W. Wang, and F. X. Jiang, "Propagation patterns of microseismic waves in rock strata during mining: an experimental study," *International Journal of Minerals, Metallurgy, and Materials*, vol. 26, no. 5, pp. 531–537, 2019.

[16] S. S. Peng, "Topical areas of research needs in ground control–a state of the art review on coal mine ground control," *International Journal of Mining Science and Technology*, vol. 25, no. 1, pp. 1–6, 2015.

[17] H. Kang, X. Zhang, L. Si, Y. Wu, and F. Gao, "In-situ stress measurements and stress distribution characteristics in underground coal mines in China," *Engineering Geology*, vol. 116, no. 3-4, pp. 333–345, 2010.

[18] M. Cai and H. Peng, "Advance of in-situ stress measurement in China," *Journal of Rock Mechanics and Geotechnical Engineering*, vol. 3, no. 4, pp. 373–384, 2011.

[19] X. Luo and P. Hatherly, "Application of microseismic monitoring to characterise geomechanical conditions in longwall mining," *Exploration Geophysics*, vol. 29, no. 3-4, pp. 489–493, 1998.

[20] S. Zhu, Y. Feng, and F. Jiang, "Determination of abutment pressure in coal mines with extremely thick alluvium stratum: a typical kind of rockburst mines in China," *Rock Mechanics and Rock Engineering*, vol. 49, no. 5, pp. 1943–1952, 2016.

[21] S. Bao, J. Cao, and S. Wang, "Vibration analysis of nanorods by the Rayleigh-Ritz method and truncated fourier series," *Results in Physics*, vol. 12, pp. 327–334, 2019.

[22] M. Zhang, J. Zhang, F. Jiang, and Z. Jiao, "Design of rib pillars in deep longwall mines based on rockburst and water-seepage prevention," *Energy Science & Engineering*, vol. 9, no. 2, pp. 256–266, 2020.

[23] M. Zhang, F. Jinag, G. Chen, Z. Jiao, H. Hu, and B. Chen, "A stope stress transfer model based on the motion state of thick and hard rock strata and its application," *Chinese Journal of Rock Mechanics and Engineering*, vol. 39, no. 7, pp. 1396–1407, 2020, in Chinese.